

SUPPORTING INFORMATION

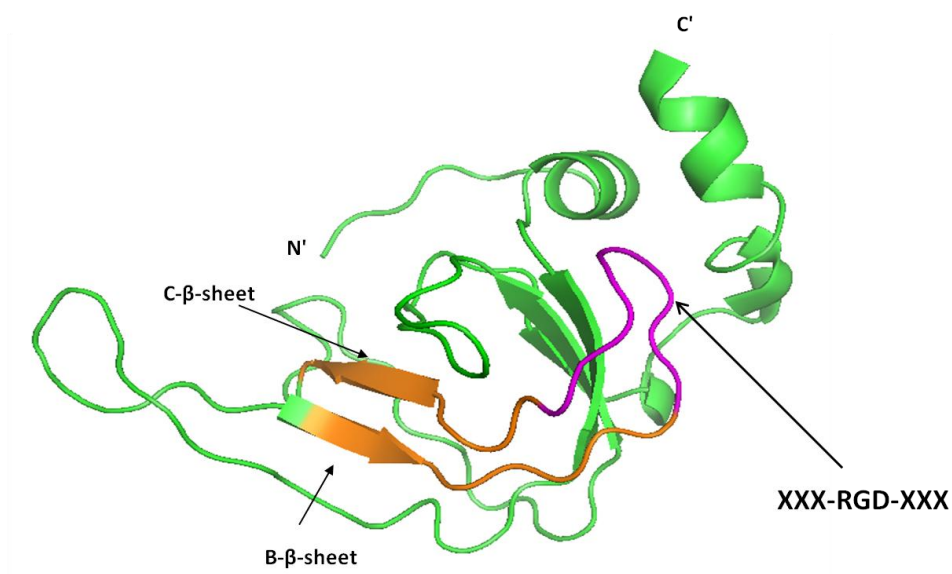


Fig. S1. N-TIMP2 structure and library position. The B-C loop is located between the B- β sheet and C- β sheet at positions 43-66 (orange and pink). The N-TIMP2_{RGD} library, located at the apex of the B-C loop, corresponding to the location of the RGD motif in fibrinogen, is located at positions 51-59 (pink). Based on 1BQQ.pdb

Supplementary Table 1. Clones identified in Sort 5.

Clone	Loop sequence*	Repetitions
Clone 1	SDQ-RGD-NAP	1
Clone 2	PEP-RGD-NAR	1
Clone 3	HTV-RGD-MPS	1
Clone 4	QEP-RGD-MPV	2
Clone 5	KTA-RGD-MPA	1
Clone 14	HGL-RGD-MPS	1
Clone 15	SMN-RGD-TIP	2
Clone 17	SQA-RGD-MPN	1
Clone 18	SEV-RGD-VPN	1

*Amino acids at positions 51-59.

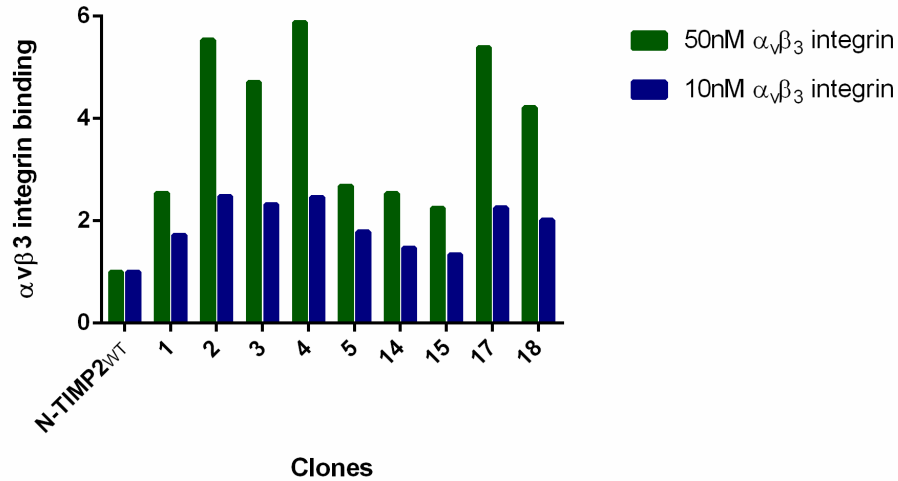


Fig. S2. Binding of the YSD N-TIMP2_{RGD} sort 5 clones to soluble integrin $\alpha_v\beta_3$. Clones binding to integrin $\alpha_v\beta_3$ were normalized to N-TIMP2_{WT}.

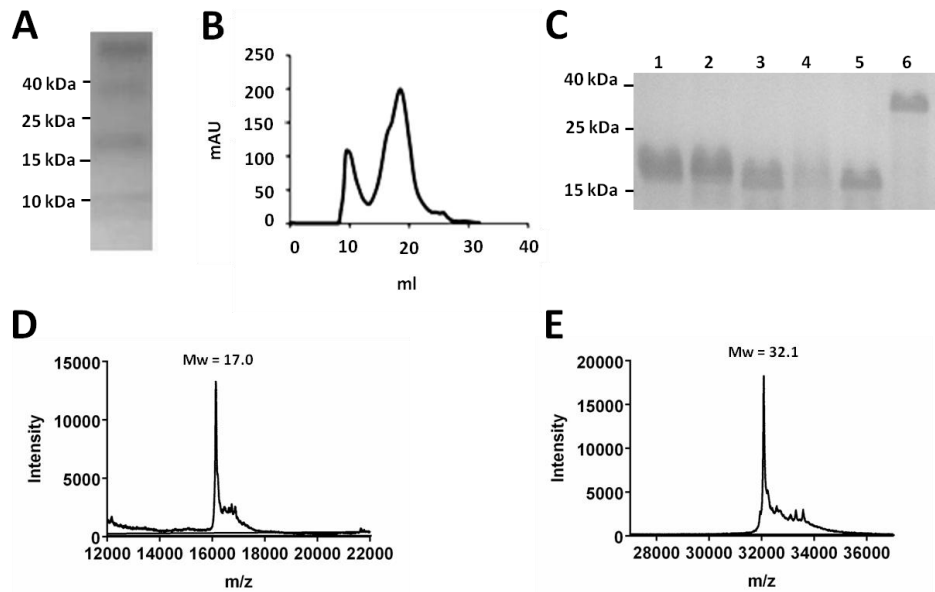


Fig. S3. N-TIMP2_{WT,RGD} purification. (A) SDS-PAGE results of N-TIMP2_{WT,RGD} (after nickel column chromatography). Four proteins of different sizes were detected, including a protein of the desired size (~17 kDa). (B) Size-exclusion purification of N-TIMP2_{WT,RGD}. The right peak represents the desired protein. (C) SDS-PAGE of all the N-TIMP2 variants (after size-exclusion chromatography). Lanes 1-6 represent N-TIMP2_{WT}, N-TIMP2_{5M}, N-TIMP2_{WT,RGD}, N-TIMP2_{5M,RGD}, Ala-N-TIMP_{WT,RGD} and N-TIMP2_{HD}, respectively. Bands of the correct sizes were detected (32 kDa for the N-TIMP2_{HD} and 17 kDa for all the other variants). (D) Mass spectrometry analysis of N-TIMP2_{WT,RGD}. (E) Mass spectrometry analysis of N-TIMP2_{HD}.

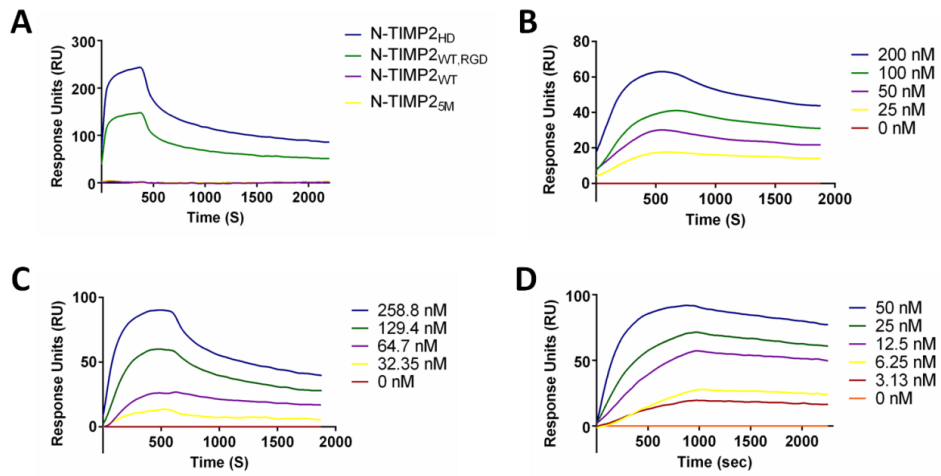


Fig. S4. Surface plasmon resonance sensorgrams. (A) N-TIMP2_{WT,RGD} and N-TIMP2_{HD} but not N-TIMP2_{WT} and N-TIMP2_{5M} bind to integrin $\alpha_v\beta_3$. Each variant (1 μM) was allowed to flow over integrin $\alpha_v\beta_3$ immobilized on a chip, and binding was detected as an increase in response units. (B) Ala-N-TIMP2_{WT,RGD} binds to integrin $\alpha_v\beta_3$. N-TIMP2_{5M,RGD} binds both integrin $\alpha_v\beta_3$ (C) and MMP-14_{CAT} (D).

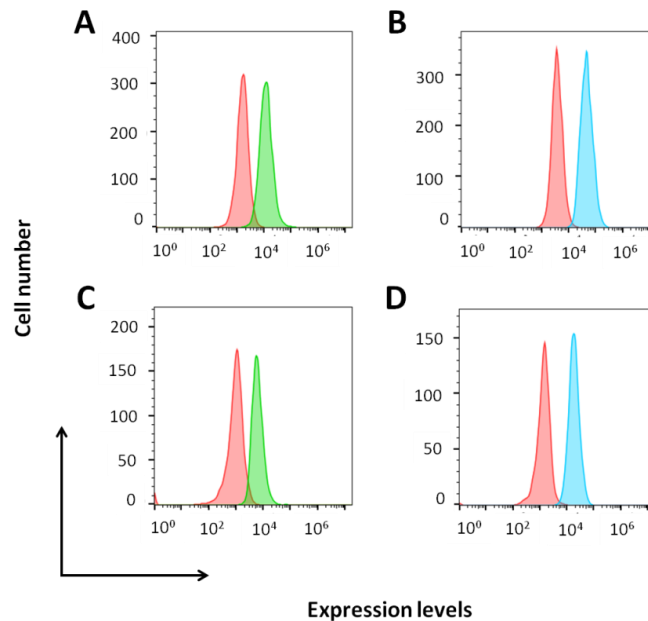


Fig. S5. Expression of MMP-14 (green) and integrin $\alpha_v\beta_3$ (blue) on TIME and U87MG cell lines compared to the control (red). Expression of MMP-14 (A) and integrin $\alpha_v\beta_3$ (B) on the U87MG cell line. Expression of MMP-14 (C) and integrin $\alpha_v\beta_3$ (D) on the TIME cell line.

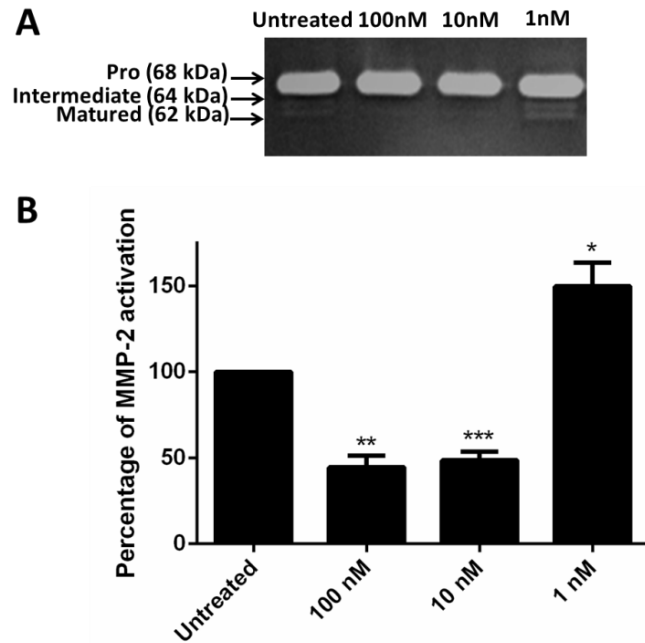


Fig. S6. Effect of the FL-TIMP2 concentration on pro-MMP-2 activation. The U87MG cell line was treated with different concentrations of FL-TIMP2 (100 nM, 10 nM and 1 nM). (A) Gelatin zymography gel results. (B) Percentage of catalytically active MMP-2. The catalytically active MMP-2, i.e. intermediate + matured forms, of each treatment was normalized to untreated cells. At high concentrations of FL-TIMP2, inhibition of pro-MMP-2 activation was observed, while at low concentrations an increase in pro-MMP-2 was detected. Error bars represent SD. Statistical analysis was performed by Student's t-test compared to the untreated control; * $P < 0.05$, ** $P < 0.005$, *** $P < 0.001$, $n = 3$.

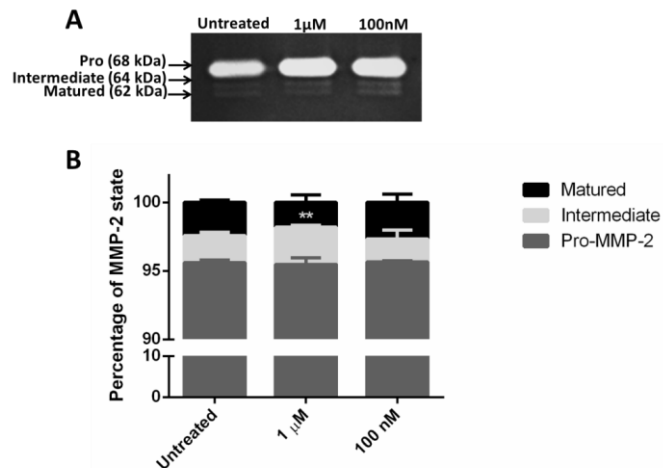


Fig. S7. Effect of cRGD treatment on the percentage of intermediate MMP-2. The U87MG cell line was treated with different concentrations of cRGD (1 μM and 100 nM). (A) Gelatin zymography gel results. (B) Quantification of the percentage of each MMP-2 form, i.e., pro/intermediate/matured [the band intensity of each MMP-2 state, i.e., pro-MMP-2 (68 kDa), intermediate MMP-2 (64 kDa) and matured MMP-2 (62 kDa), was divided by the total band intensity of all the MMP-2 forms, i.e., pro+intermediate+ matured MMP-2]. Processing of the intermediate form was significantly inhibited by 1 μM of cRGD. Error bars represent SEM. Statistical analysis was performed by Student's t-test compared to the untreated control; ** $P < 0.005$, $n = 3$.